ChemPhysChem

Chemistry Europe
European Chemical Societies Publishing
ChemPhysChem

RESEARCH ARTICLE OPEN ACCESS

Evaluation of Sunflower Sprout Extract as a Bioinspired Support to UV Filtration

Michael Hymas[1] | Marc Fischer[2] | Stéphane Poigny[2] | Vasilios G. Stavros[1]

[1]School of Chemistry, University of Birmingham, Birmingham, United Kingdom | [2]Mibelle Group Biochemistry, Mibelle AG, Buchs, Switzerland

Correspondence: Michael Hymas (m.hymas@bham.ac.uk) | Vasilios G. Stavros (v.stavros@bham.ac.uk)

Received: 22 September 2025 | **Revised:** 4 February 2026 | **Accepted:** 4 February 2026

Keywords: biomimetic | natural extract | photophysics | photoprotection | sunscreen

ABSTRACT

The photochemistry of a commercial sunflower sprout extract was compared to that of pure chlorogenic acid (3-*O*-caffeoylquinic acid), a key photoprotective species found in the extract. Steady-state and time-resolved spectroscopy experiments revealed virtually equivalent photodynamics between aqueous solutions of the sunflower extract and chlorogenic acid, namely ~5 picosecond nonradiative deactivation following UV photoexcitation. For chlorogenic acid, this nonradiative deactivation is achieved by relaxation through a conical intersection, mediated through rotation around the caffeoyl C═C double bond. These photophysical similarities tentatively justify the use of the unpurified sprout extract for use in UV photoprotective formulations and demonstrate that the environmental complexity conferred by the presence of other phytochemical constituents in the extract does not impede the relaxation mechanism of chlorogenic acid.

1 | Introduction

Hydroxycinnamic acids are ubiquitous in nature, found in fruits, vegetables, and grains [1]. Chlorogenic acid (otherwise known as 3-*O*-caffeoylquinic acid to distinguish it from its 4-*O*- and 5-*O*- isomers, and hereafter abbreviated to 3-3-CGA), a well-known hydroxycinnamic acid, is known to be an effective antioxidant and carcinogenic inhibitor [1]. Motivated by its phytochemical abundance and appropriate sunscreen properties (e.g., sun protection factor (SPF), critical wavelength (λ_c), and UVA/UVB ratio) [2], 3-CGA has been previously studied in terms of its excited-state nonradiative deactivation (NRD) mechanism [3]. 3-CGA's UV filter properties arise from absorption to a $\pi\pi^*$ (S_1) state, which is weakly emissive, followed by relaxation to the ground (S_0) state through a S_1/S_0 conical intersection (CI). According to calculated potential energy surfaces (PES), propagation through this CI involves rotation around the central caffeoyl C ═ C double bond, thereby generating either the starting *trans* or *cis* photoproduct isomer in the ground state, the latter of which is somewhat disfavored due to a barrier in the S_1 [3]. In light of its UV protective properties, previous research has endorsed 3-CGA's inclusion in sunscreen formulations [2, 4, 5].

In this study, we have explored the photochemistry of a major phytochemical source of 3-CGA, namely a commercial extract from the sprouts of sunflower, *Helianthus annuus* [6]. Hydroxycinnamic acids, including 3-CGA, have been identified, by ultraperformance liquid chromatography (UPLC), in appreciable abundance in these sprouts.

We are interested in the applicability of "crude" and abundant natural extracts supporting UV filtration in sunscreen formulations and how other components in extracts might influence the photoprotection mechanisms of 3-CGA, if at all. To this end, we have approached analyzing the sunflower sprouts extract by a mixed steady-state and time-resolved spectroscopic scheme. We look at the extract (and an analytical reference of 3-CGA) using UV–visible absorption spectroscopy and femtosecond transient electronic absorption spectroscopy (fs-TEAS) to determine its in vitro UV protection properties and ultrafast photochemistry. Aqueous 3-CGA and the extract were found to exhibit very similar ultrafast properties and comparable steady-state UV

properties, despite their compositional disparity, supporting the viability of the crude product for sunscreen applications.

2 | Experimental Methods

2.1 | Extract Preparation

The *Helianthus annuus* extract was prepared as follows: hot water extraction was undertaken on the fresh sprouts for 5 h, then 15% ethanol was added, and the solution filtered to remove all remaining solid plant matter, yielding "Mibexol SB pf." This solution (2 kg) was then lyophilized by a rotary evaporator to yield the dry extract "Mibexol SB pf Lyo" (22 g, or 1.1% dry content in solution), used for spectroscopy experiments.

2.2 | UPLC

All solvents used were of high performance liquid chromatography (HPLC) grade unless otherwise stated. Mibexol SB pf was analyzed by UPLC (Acquity UPLC TUV Detector, Waters Corporation). 2 µL of filtered extract (WICOM PVDF filter vials 0.45 µm) was injected without dilution *versus* reference standards of 3-CGA (Fluka, 25 700, Lot No. 1 387 241 22408172) and 5-*O*-caffeoylquinic acid (5-CGA) (Sigma–Aldrich, 94 419, Lot No. WXBD0790V) with approximate concentrations: 5, 25, 50, and 100 µg/g dissolved in ethanol/water (Milli-Q) 1:1 (w/w). A reference standard for 4-*O*-caffeoylquinic acid (4-CGA) was not available, so the response factor of 3-CGA was used in experiments due to its absorptive similarity at 280 nm [7]. Elution of all chlorogenic acids (e.g., 3–, 4- and 5-CGA) occurred within the isocratic window (<4.5 min).

2.3 | Steady-State Optical Spectroscopy

For spectroscopic measurements (excluding extinction coefficients), aqueous solutions of 3-CGA (PhytoLab, used without further purification) and Mibexol SB pf Lyo were made up to ~ 0.5 absorption at 324 nm. Solutions were covered with foil during storage to exclude ambient light and maintained at 21 ± 1°C.

To assess solar photostability, UV–visible absorption spectra were recorded before and after 2 h' irradiation under a simulated solar spectrum (LCS-100, Spectra-Physics).

Steady-state UV–visible absorption spectra were recorded using a Cary 60 UV/Vis spectrophotometer, in a 1 mm quartz cuvette.

2.4 | Fs-TEAS

Fs-TEAS experiments are outlined in detail elsewhere [8], so only details specific to our experiments are described herein. The "pump" excitation wavelength was set to 324 nm, to coincide with maximal absorption in aqueous 3-CGA (see Figure 1). The pump pulse energy was ~500 nJ, and the spot size ~350 µm at the sample. The "probe" pulse was a white light supercontinuum that spanned ~320–720 nm, generated by focusing an 800 nm fundamental beam into a translating CaF_2 crystal. Pump–probe time delay, Δt, was controlled by a motorized delay stage (<2.5 ns). A 1 mm quartz cuvette, containing the aqueous solution, was translated in a plane perpendicular to the beam

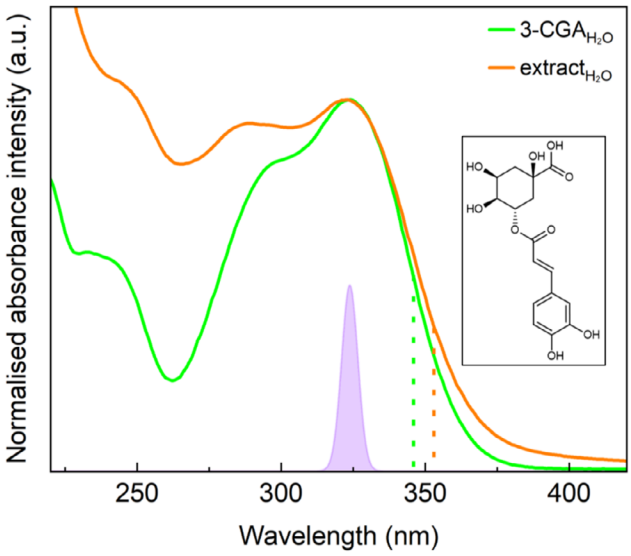

FIGURE 1 | UV–visible absorption spectra of aqueous Mibexol SB pf Lyo (orange) and pure 3-CGA (green) at 21°C. Critical wavelengths (dashed vertical) and approximate pump profile used in fs-TEAS experiments (purple shaded) are also shown. Inset: structure of 3-CGA.

geometry, to avoid interrogating any possible photoproduct with subsequent pump-probe pulse pairs.

Collected transient absorption spectra were fit with a sequential global model, implemented via the software package Glotaran [9]. Heatmaps in Figure 2 were treated using the KOALA software to model and correct dispersion [10].

An instrument response function (IRF) was evaluated by fitting a kinetic transient absorption trace of water under equivalent experimental conditions (see Figure S3).

3 | Results and Discussion

3.1 | Results

3.1.1 | UPLC

Results from UPLC are summarized in Table 1. Of the three structural isomers of chlorogenic acid, 3-CGA itself is the least abundant in Mibexol SB pf, accounting for 28.2% of the caffeoylquinic acid content.

3.1.2 | Steady-State UV–visible Absorption Properties

Initially, comparative UV–visible absorption spectra of aqueous 3-CGA and Mibexol SB pf Lyo were collected (Figure 1), showing a similar red-edge absorption profile, peaking at ~324 nm. It was determined by Cornard et al. that 3-CGA's absorption maximum at 324 nm corresponds to a LUMO ← HOMO transition (S_1 $^1\pi\pi^*$) whose density is primarily focused around the caffeoyl moiety. Slight absorption at >350 nm arises from a lower lying transition, with much diminished oscillator strength, which becomes enhanced at higher pH [11].

Parameters based exclusively on the shape of the extract solution's absorption profile are here presented (i.e., critical wavelength, solar photostability, UVA ratio). No SPF or UVA

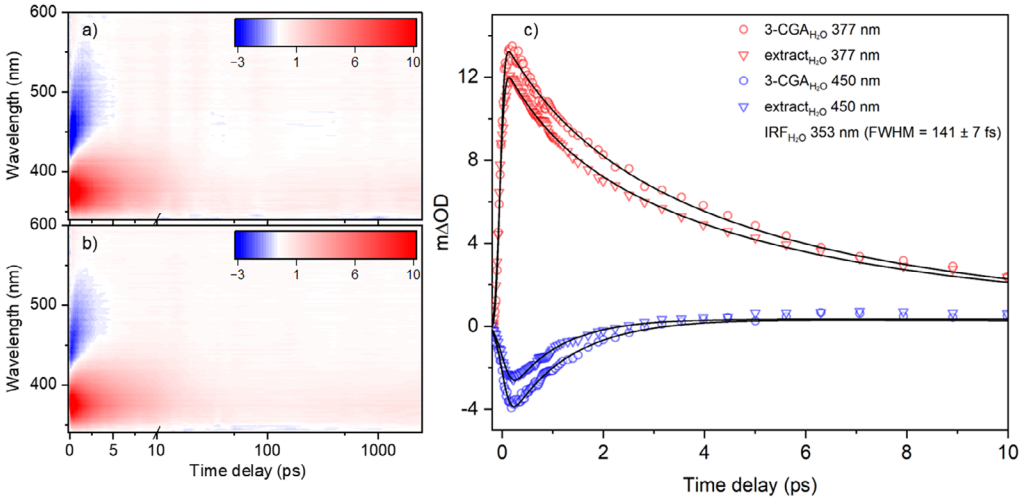

FIGURE 2 | Heatmaps of collected TEA spectra for aqueous (a) 3-CGA and (b) Mibexol SB pf Lyo, following photoexcitation at 324 nm. (c) Kinetic transient absorption traces at 377 nm (red) and 450 nm (blue), with fits from global sequential fitting overlaid (black).

TABLE 1 | UPLC data (retention time (tR) and amounts) of chlorogenic acid isomers in Mibexol SB pf.

Analyte	tR, min	Amount, μg/g	%
5-CGA (5-*O*-caffeoylquinic acid)	1.869	52.76	29.3
4-CGA (4-*O*-caffeoylquinic acid)	3.606	76.55	42.5
3-CGA (3-*O*-caffeoylquinic acid)	3.843	50.80	28.2

protection are reported, as these qualities depend on application (thickness, etc.) [12].

Critical wavelength λ_c [12] of aqueous Mibexol SB pf Lyo was calculated according to the following equation:

$$\int_{290}^{\lambda_c} A(\lambda)d\lambda = 0.9\int_{290}^{400} A(\lambda)d\lambda \quad (1)$$

yielding $\lambda_c = 353$ nm. This is a shorter wavelength than that determined for aqueous 3-CGA (372 nm) by Rivelli et al.; it should be noted, however, that our analysis of aqueous 3-CGA yielded $\lambda_c = 347$ nm (see Figure 1). The European Commission and the US Food and Drug Administration (FDA) rule that only sunscreens whose $\lambda_c > 370$ nm can be described as "broad-spectrum" absorbers, indicating good protection against UVA [13, 14].

Photostability under a simulated solar spectrum (see Figure S1) was measured. An area under curve index (AUCI) was determined for aqueous Mibexol SB pf Lyo and 3-CGA according to the following equation:

$$\text{AUCI} = \frac{\int_{290}^{400} A_0(\lambda)d\lambda}{\int_{290}^{400} A_{2h}(\lambda)d\lambda} \quad (2)$$

where $A_{2h}(\lambda)$ is absorbance following 2 h solar irradiation. An AUCI of 83.5% was calculated for the extract and 88.8% for 3-CGA, indicating 3-CGA is marginally more stable than Mibexol SB pf Lyo.

The UVA ratio (i.e., integrated ratio of total absorption in the UVA to that in the UVB, following 2 h solar irradiation) was calculated by the following [15]:

$$\frac{\text{UVA}}{\text{UVB}} = \frac{\int_{320}^{400} A(\lambda)d\lambda}{\int_{290}^{320} A(\lambda)d\lambda} = 1.05 \quad (3)$$

According to the Boots star rating system [16], this solution therefore provides 5-star protection (i.e., UVA ratio ≥ 0.9). By comparison, Rivelli et al. reported a UVA ratio of 0.81 (4-star protection, i.e., 0.9 > UVA ratio ≥ 0.8) for aqueous 3-CGA [2].

A weight/volume extinction coefficient for aqueous Mibexol SB pf Lyo at 324 nm was determined as $3.54 \pm 0.04\ g^{-1}\ dm^3\ cm^{-1}$ (see Figure S2); in comparison, an equivalent treatment of aqueous 3-CGA (using a molar extinction coefficient from literature [17]) yielded $53.1 \pm 0.8\ g^{-1}\ dm^3\ cm^{-1}$.

3.1.3 | FS-TEAS

To determine the differences between the ultrafast (ps) behavior of the extract versus pure 3-CGA, fs-TEAS was undertaken on aqueous solutions of each. Figure 2 shows heatmaps of collected TEA spectra following photoexcitation of aqueous 3-CGA (a) and Mibexol SB pf Lyo (b) at 324 nm and kinetic traces at selected wavelengths (c). Global sequential fitting was undertaken [9], extracted lifetimes from which are presented in Table 2.

TABLE 2 | Lifetimes extracted from global sequential fit of collected TEA data for aqueous 3-CGA and Mibexol SB pf Lyo. Half the extracted IRF is reported as the error, except in cases where error from the fitting process is greater.

	Lifetime, ps		
System	τ_1	τ_2	τ_3
3-CGA$_{H_2O}$	1.25 ± 0.070	5.16 ± 0.070	>2500
Mibexol SB pf Lyo$_{H_2O}$	0.98 ± 0.070	5.06 ± 0.205	>2500

Virtually identical dynamics were seen in each case, with quantitatively similar lifetimes extracted. The following analysis therefore applies to TEA data of both aqueous systems. The intense positive absorption feature at ~375 nm is assigned to vertical excited-state absorption (ESA) from the initially promoted state, identified previously as S_1 (i.e., $S_{n>1} \leftarrow S_1$) [11]. The sequential decay lifetimes associated with this signal are ~1 and ~5 ps (τ_1 and τ_2), although a small component persists beyond our maximum pump-probe time delay ($\tau_3 > 2.5$ ns). The spectral profile of this feature remains largely unperturbed, only diminishing in signal strength, suggesting that the relative energy gap between involved states (i.e., S_1 and $S_{n>1}$) remains constant. Conversely, the broad negative feature originating at ~450 nm, assigned as stimulated emission (SE) from S_1 to the ground (S_0) state, redshifts within the initial ~1 ps following photoexcitation. This spectral evolution implies a steeply inclined PES along the path of excited state relaxation, as the vertical gap between S_1 and S_0 evidently reduces with time. That this SE signal decays within ~1 ps indicates that the transition becomes optically dark somewhere along the relaxation coordinate and does not subsequently recover oscillator strength. Finally, the edge of a ground-state bleach (GSB) signal, originating from depletion of S_0 population, can be seen at <350 nm, which persists to the end of our experiment, indicating some portion of unrecovered ground state 3-CGA.

3.2 | Discussion

3.2.1 | Steady State UV–visible Absorption Properties

As has been identified here, the predominant absorbing species in extracts of *Helianthus annuus* sprouts are isomers of 3-CGA. The extract exhibits an identical UV absorption maximum at 324 nm (albeit with a ~15-fold lower w/v extinction coefficient), with slightly broader absorption on the peak's red edge, possibly due to scattering from undissolved matter and evidenced by a heightened UVA ratio, along with increased absorption at wavelengths shorter than this. This latter fact suggests the sprout extracts contain other chromophores than 3-CGA, absorbing in the vicinity, which could demonstrate different photochemistry. The presence of other similarly conjugated hydroxycinnamoyl substituted esters [18] in the extract explains the lack of definition in absorption maximum versus pure 3-CGA. Generally, this broadened absorption into the UVA is desirable for sunscreen applications [12].

The phenolic profile of sunflower extracts varies depending on the plant's growth stage at harvest [19]. Many related properties of the extract (e.g., electronic absorption profile, antioxidant ability) are therefore similarly sensitive to growth stage, so it is possible that the photoprotective ability of *Helianthus annuus* varies with crop age.

3.2.2 | FS-TEAS

The results from fs-TEAS demonstrate negligible differences between the bulk ultrafast properties of aqueous 3-CGA and the sunflower sprout extract. The following interpretation, although undertaken with 3-CGA in mind, can therefore be extended to TEA data of both aqueous systems. As has been identified previously in similar analytes, the ~1 ps lifetime (τ_1) extracted from both fs-TEAS experiments is attributed to a convolution of several excited state processes in $^1\pi\pi^*$, including solvation, rapid geometric rearrangement out of the Franck–Condon region, and initial intramolecular vibrational redistribution [3, 20–23]. τ_1 also captures artifacts from the IRF (see Figure S3). τ_2 then reflects further vibrational cooling in $^1\pi\pi^*$ and population transfer to S_0 through a $^1\pi\pi^*/S_0$ conical intersection, mediated by a *trans-cis* isomerization coordinate [3]. τ_3 reflects unrecovered GSB and residual ESA. Due to the appreciable content of 4- and 5-CGA in the sunflower sprout extract (see Table 2) and the similarity between the two aqueous systems' fs-TEAS results, we can infer that the ultrafast behavior of these isomers following photoexcitation is strongly comparable to that of 3-CGA. The above analysis qualitatively agrees with the findings of Wang et al. for 3-CGA in methanol, albeit with substantially shorter lifetimes extracted in ours [3]; this discrepancy is potentially due to enhanced vibrational cooling rates by interaction with the water network in our experiments, an environmental effect in NRD observed elsewhere [24, 25]. In the case of the sunflower extract, a plethora of photoproducts is likely generated, including *cis* forms of any 3-CGA isomers.

The combined findings from steady-state and time-resolved spectroscopies suggest that 3-CGA's (and its isomers') photodynamics are largely unaffected by the extract's other constituents or that these other constituents exhibit equivalent ultrafast photochemistry. It is probable that other isomers of 3-CGA (e.g., 4- and 5-caffeoylquinic acid) undergo analogous NRD pathways. These results therefore valorize the use of "crude" natural extracts for use in photoprotective formulations, at least from a photometric standpoint, without the requirement for lengthy and expensive purification stages. This echoes the findings of Abiola et al. vis-à-vis sinapoyl malate in *Lepidium sativum* sprouts extracts [26]. Any other deleterious (or beneficial) properties of the extract would need to be evaluated separately, either toxicologically or chemically, before it was commercialized.

4 | Conclusion

We have compared the photochemistry of 3-*O*-caffeoylquinic acid (3-CGA) and an extract from sprouts of the common sunflower, *Helianthus annuus*, whose major chromophores are isomers of chlorogenic acid (including 3-CGA itself). Our findings indicate there are minimal differences in the photoprotective ability of each, particularly from a time-resolved perspective, and that the nonradiative relaxation mechanism of 3-CGA in each, following UV photoexcitation, is dominated by either a full or aborted *trans-cis* isomerization in the caffeoyl moiety. The similarity between bulk photochemistry between purified and crude samples therefore motivates future work in investigating the photoprotective characteristics of other natural extracts, including *Helianthus annuus* at other growth stages, the use of which in sunscreen formulations would be significantly cheaper and less wasteful.

Acknowledgments

The authors would like to acknowledge the Warwick Centre for Ultrafast Spectroscopy (https://warwick.ac.uk/fac/sci/wcus) for use of the Cary 60 UV/Vis Spectrometer and the fs-TEAS set-up. M.H. was supported by NERC CENTA2 (grant no. NE/S007350/1). V.G.S. thanks the Royal Society for a Royal Society Industry Fellowship. The authors would like

to thank Mibelle Group Biochemistry for supplying the 3-CGA and sunflower sprouts extract samples.

Funding

This study was supported by Natural Environment Research Council (NE/S007350/1).

Conflicts of Interest

The authors declare no conflicts of interest.

Data Availability Statement

The data that support the findings of this study are available from the corresponding author upon reasonable request.

References

1. N. J. Kang, K. W. Lee, B. J. Shin, et al., "Caffeic Acid, a Phenolic Phytochemical in Coffee, Directly Inhibits Fyn Kinase Activity and UVB-Induced COX-2 Expression," *Carcinogenesis* 30, no. 2 (2008): 321–330, https://doi.org/10.1093/carcin/bgn282.

2. D. P. Rivelli, C. A. H. Filho, R. L. Almeida, C. D. Ropke, T. C. H. Sawada, and S. B. M. Barros, "Chlorogenic Acid UVA–UVB Photostability," *Photochemistry and Photobiology* 86, no. 5 (2010): 1005–1007, https://doi.org/10.1111/j.1751-1097.2010.00776.x.

3. M. Wang, Y. Shi, Y. Guo, et al., "Nonadiabatic Dynamics Mechanisms of Natural UV Photoprotection Ompounds Chlorogenic Acid and Isochlorogenic Acid a: Double Conjugated Structures but Single Photoexcited Channel," *Journal of Molecular Liquids* 324 (2021): 114725, https://doi.org/10.1016/j.molliq.2020.114725.

4. B. Choquenet, C. Couteau, E. Paparis, and L. J. M. Coiffard, "Molecular Families with Sunscreen Potential: Determining Effectiveness with an In Vitro Method," *Natural Product Communications* 4, no. 2 (2009): 227–230.

5. J. W. Cha, M. J. Piao, K. C. Kim, et al., "The Polyphenol Chlorogenic Acid Attenuates UVB-Mediated Oxidative Stress in Human HaCaT Keratinocytes," *Biomolecules & Therapeutics* 22, no. 2 (2014): 136–142, https://doi.org/10.4062/biomolther.2014.006.

6. S. Guo, Y. Ge, and K. Na Jom, "A Review of Phytochemistry, Metabolite Changes, and Medicinal Uses of the Common Sunflower Seed and Sprouts (Helianthus Annuus L)," *Chemistry Central Journal* 11, no. 1 (2017): 95, https://doi.org/10.1186/s13065-017-0328-7.

7. I. Tomac, L. Jakobek, and M. Šeruga, "Chromatographic and Voltammetric Characterization of Chlorogenic Acids in Coffee Samples," *Croatica Chemica Acta* 91, no. 4 (2018): 501, https://doi.org/10.5562/cca3439.

8. T. T. Abiola, N.d N. Rodrigues, C. Ho, et al., "New Generation UV-A Filters: Understanding Their Photodynamics on a Human Skin Mimic," *ournal of Physical Chemistry Letters* 12, no. 1 (2021): 337–344, https://doi.org/10.1021/acs.jpclett.0c03004.

9. J. J. Snellenburg, S. Laptenok, R. Seger, K. M. Mullen, and I. H. Mvan Stokkum, "Glotaran: A Java-Based Graphical User Interface for the R Package TIMP," *Journal of Statistical Software* 49 (2012): 1–22, https://doi.org/10.18637/jss.v049.i03.

10. M. P. Grubb, A. J. Orr-Ewing, and M. N. R. Ashfold, "KOALA: A Program for the Processing and Decomposition of Transient Spectra," *Review of Scientific Instruments* 85, no. 6 (2014): 064104, https://doi.org/10.1063/1.4884516.

11. J.-P. Cornard, C. Lapouge, L. Dangleterre, and C. Allet-Bodelot, "Complexation of Lead(II) by Chlorogenic Acid: Experimental and Theoretical Study," *Journal of Physical Chemistry A* 112, no. 48 (2008): 12475–12484, https://doi.org/10.1021/jp805463p.

12. B. L. Diffey, P. R. Tanner, P. J. Matts, and J. F. Nash, "In Vitro Assessment of the Broad-Spectrum Ultraviolet Protection of Sunscreen Products," *Journal of the American Academy of Dermatology* 43, no. 6 (2000): 1024–1035, https://doi.org/10.1067/mjd.2000.109291.

13. B. Diffey, "Spectral Uniformity: A New Index of Broad Spectrum (UVA) Protection," *International Journal of Cosmetic Science* 31, no. 1 (2009): 63–68, https://doi.org/10.1111/j.1468-2494.2008.00471.x.

14. S. Q. Wang, H. Xu, J. W. Stanfield, U. Osterwalder, and B. Herzog, "Comparison of Ultraviolet A Light Protection Standards in the United States and European Union through In Vitro Measurements of Commercially Available Sunscreens," *Journal of the American Academy of Dermatology* 77, no. 1 (2017): 42–47, https://doi.org/10.1016/j.jaad.2017.01.017.

15. A. Springsteen, R. Yurek, M. Frazier, and K. F. Carr, "In Vitro Measurement of Sun Protection Factor of Sunscreens by Diffuse Transmittance1," *Analytica Chimica Acta* 380, no. 2 (1999): 155–164, https://doi.org/10.1016/S0003-2670(98)00577-7.

16. M. Manikrao Donglikar, and S. Laxman Deore, "Sunscreens: A Review," *Pharmacognosy Journal* 8, no. 3 (2016): 171–179, https://doi.org/10.5530/pj.2016.3.1.

17. A. Belay and A. V. Gholap, "Characterization and Determination of Chlorogenic Acids (CGA) in Coffee Beans by UV-Vis Spectroscopy," *African Journal of Pure and Applied Chemistry* 3, no. 11 (2009): 34–240, https://doi.org/10.5897/AJPAC.9000029.

18. G. M. Weisz, D. R. Kammerer, and R. Carle, "Identification and Quantification of Phenolic Compounds from Sunflower (Helianthus Annuus L.) Kernels and Shells by HPLC-DAD/ESI-MSn," *Food Chemistry* 115, no. 2 (2009): 758–765, https://doi.org/10.1016/j.foodchem.2008.12.074.

19. F. Gai, M. Karamać, M. A. Janiak, R. Amarowicz, and P. G. Peiretti, "Sunflower (Helianthus annuus L.) Plants at Various Growth Stages Subjected to Extraction—Comparison of the Antioxidant Activity and Phenolic Profile," *Antioxidants* 9, no. 6 (2020): 535, https://doi.org/10.3390/antiox9060535.

20. Y. Shi, X. Zhao, C. Wang, et al., "Ultrafast Nonadiabatic Photoisomerization Dynamics Mechanism for the UV Photoprotection of Stilbenoids in Grape Skin," *Chemistry – An Asian Journal* 15, no. 9 (2020): 1478–1483, https://doi.org/10.1002/asia.202000219.

21. X. Zhao, F. Ji, Y. Liang, et al., "Theoretical and Spectroscopic Investigation on Ultrafast Nonadiabatic Photoprotective Mechanism of Novel Ultraviolet Protective Compounds Inspired by Natural Sunscreens," *Journal of Luminescence* 223 (2020): 117228, https://doi.org/10.1016/j.jlumin.2020.117228.

22. M. D. Horbury, A. L. Flourat, S. E. Greenough, F. Allais, and V. G. Stavros, "Investigating Isomer Specific Photoprotection in a Model Plant Sunscreen," *Chemical Communications* 54, no. 8 (2018): 936–939, https://doi.org/10.1039/C7CC09061G.

23. J. Luo, Y. Liu, S. Yang, A. L. Flourat, F. Allais, and K. Han, "Ultrafast Barrierless Photoisomerization and Strong Ultraviolet Absorption of Photoproducts in Plant Sunscreens," *Journal of Physical Chemistry Letters* 8, no. 5 (2017): 1025–1030, https://doi.org/10.1021/acs.jpclett.7b00083.

24. J. M. Woolley, N. D. N. Rodrigues, J. M. Toldo, et al., "Molecular Heaters: A Green Route to Boosting Crop Yields?," *Physical Chemistry Chemical Physics* 27, no. 14 (2025): 7375–7382, https://doi.org/10.1039/D4CP04803B.

25. J. M. Woolley, M. Staniforth, M. D. Horbury, G. W. Richings, M. Wills, and V. G. Stavros, "Unravelling the Photoprotection Properties of Mycosporine Amino Acid Motifs," *Journal of Physical Chemistry Letters* 9, no. 11 (2018): 3043–3048, https://doi.org/10.1021/acs.jpclett.8b00921.

26. T. T. Abiola, N. Auckloo, J. M. Woolley, C. Corre, S. Poigny, and V. G. Stavros, "Unravelling the Photoprotection Properties of Garden

Cress Sprout Extract," *Molecules* 26, no. 24 (2021): 7631, https://doi.org/10.3390/molecules26247631.

27. M. Hymas, J. Eller, M. Salehi, R. Omidyan, S. Poigny, and V. G. Stavros, "Excited State Deactivation in Phytochemical Flavonoids: Astragalin and Kaempferol," *Physical Chemistry Chemical Physics* 27, no. 30 (2025): 15895–15905, https://doi.org/10.1039/D5CP01895A.

Supporting Information

Additional supporting information can be found online in the Supporting Information section. The authors have cited additional references within the Supporting Information [17, 27]. **Supporting Fig. S1:** Absorption spectra of aqueous Mibexol SB pf Lyo (orange) and 3-CGA (green) before (solid) and after (dashed) 2 h irradiation under a simulated solar spectrum (normalized counts: pink). **Supporting Fig. S2:** (a) Calibration plot for weight/volume extinction coefficient of aqueous Mibexol SB pf Lyo at 324 nm; (b) absorption spectra of aqueous Mibexol SB pf Lyo (orange) and 3-CGA[1] (green) scaled by weight/volume extinction coefficient at 324 nm. **Supporting Fig. S3:** Kinetic transient absorption trace at 353 nm of H_2O photoexcited at 324 nm (gray) and fit IRF (141 ± 7 fs) overlaid (pink, as included in Figure 2). **Supporting Table S1:** UPLC instrument operation details. **Supporting Table S2:** Gradient for purging column.